1 Supplementary material

Two simple simulation cases, including only one source in one of the slurry pits, have been included in the supplementary material. The two cases differ by the presence of an external source outside the inversion domain. This will cross-contaminate the PAC measurements and make it significantly harder to quantify sources inside the inversion domain.

1.1 Case 1 - single emission source

Figure 1 shows the true and reconstructed concentration and source distributions for supplementary simulation case 1. The concentration and source distributions are illustrated at times 15, 30, 45, and 60 min of the simulations (rows). Figure 2 shows the corresponding integrated source distributions as time-evolving emission rates with 95 % posterior credibility intervals for the unconstrained (top) and the constrained source model (bottom). Finally, Fig. 3 shows the simulated vs. the estimated PAC measurements for the single source case.

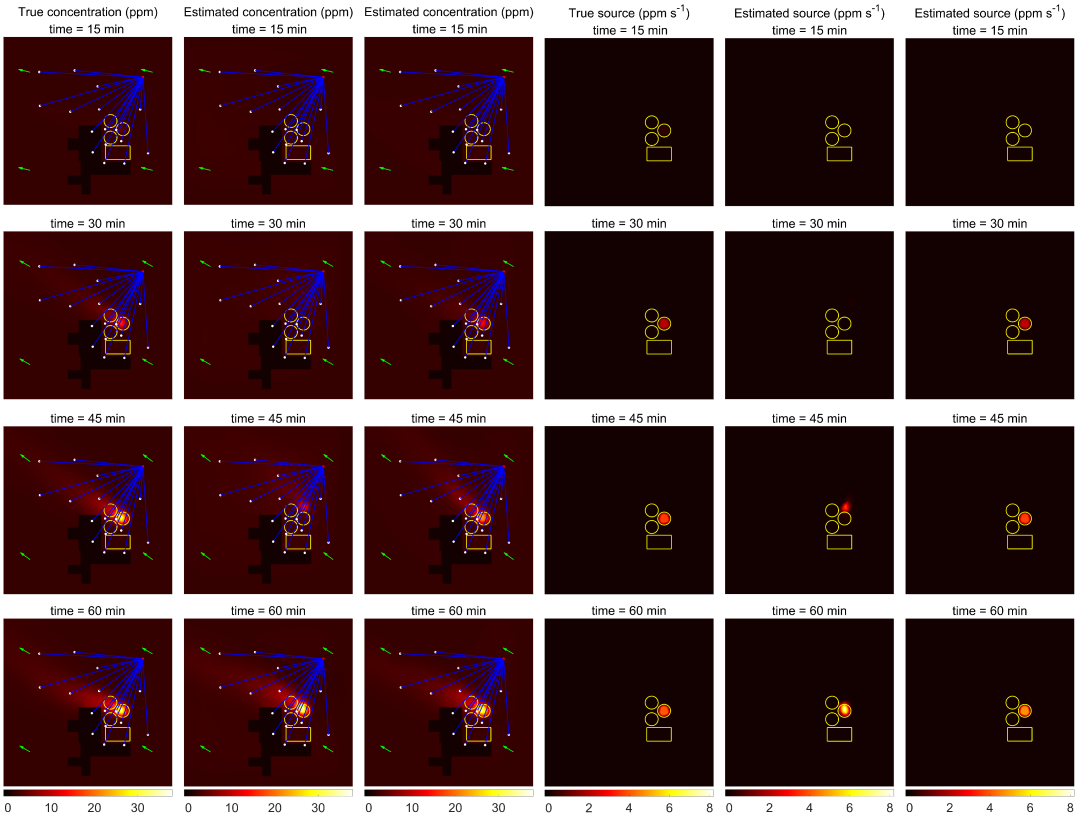

Figure 1. Case 1 - First column) true concentration distribution at different time instants. The wind direction at each time is shown with green vectors. Second column) estimated concentration distribution using the unconstrained model. Third column) estimated concentration distribution using the constrained model. Fourth column) true source distribution. Fifth column) estimated source distribution using the unconstrained model. Sixth column) estimated source distribution using the constrained model.

The reconstructed concentration distributions in Fig. 1 using the unconstrained and constrained source models (second and third columns) show good correspondence with the true concentration distribution (first column). The reconstructed gas plumes capture the transport of gas in the direction of the velocity field marked with green vectors. In the reconstructed source distribution using the unconstrained source model (fifth column), the peak source value is approximately double that of the

15 true source. This is because the true source distribution is a piecewise constant function with its support fully contained in the slurry pit. The unconstrained source model, however, models the source distribution as a smooth function.

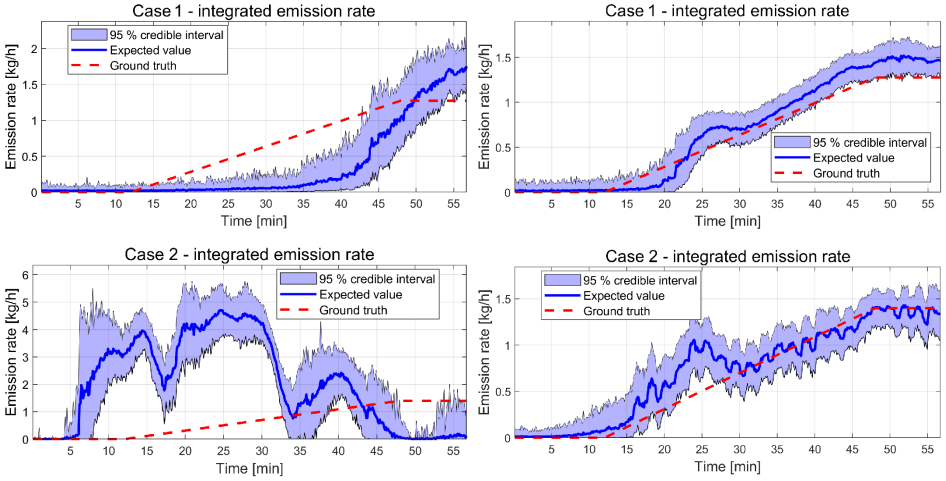

Figure 2. Integrated source distributions in kg h^{-1} for all simulation cases using the unconstrained (left column) and the constrained source evolution models (right column).

Figure 5 shows the estimated integrated emission rates for both simulation cases using the unconstrained and the constrained source evolution models. The first row shows the integrated emission rates for simulation case 1. Using the unconstrained source model, the 95 % posterior credibility intervals contain the true integrated emission rate about 40 % of the time. For the
20 constrained source model, the true integrated emission rate is estimated within the 95 % posterior credibility intervals at all times.

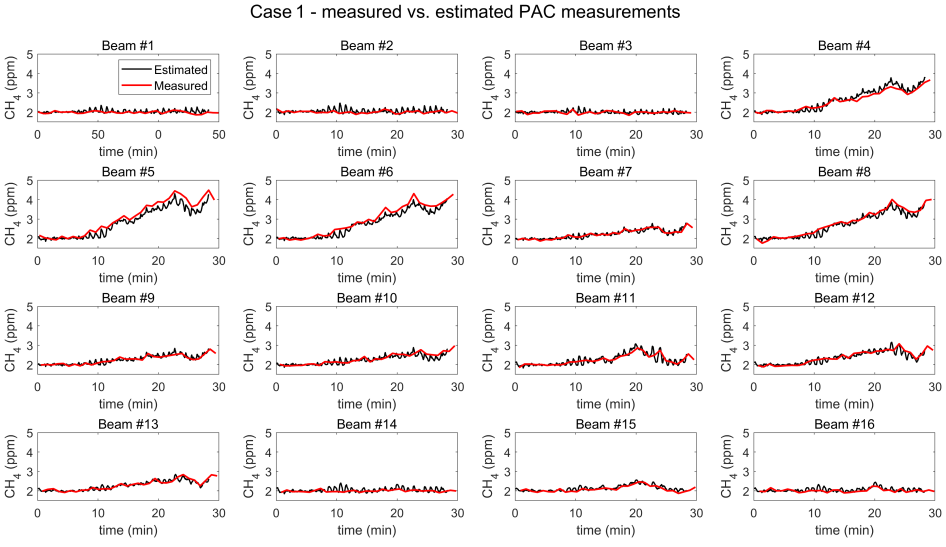

Figure 3. Case 1 - Measured (from forward simulation) and estimated (from inversion) PAC measurements using the constrained model.

1.2 Case 2 - single source with external input

Figure 4 shows the true and reconstructed concentration and source distributions for supplementary simulation case 2. The concentration and source distribution estimates in Fig. 4 show that the unconstrained source model (second and fifth columns) does not recognize that gas enters the domain through the input boundary and does not detect the true source. Instead, the model tries to explain the measured PAC data in Fig. 5 by creating sources at the edge of the support of the source distribution. The unconstrained source model performs poorly when external sources cross-contaminate the PAC data. In this simulation case, the constrained source model effectively mitigated the impact of external gas sources, avoiding spurious false sources near the boundary.

The bottom row of Fig. 2 shows the estimated integrated emission rates from the unconstrained and constrained source evolution models. The constrained source model detects the source after 15-20 minutes, while the true source appears after 12 minutes. The constrained source model gives a good estimate of the integrated emission rate, and the true integrated emission rate is contained within the 95 % posterior credible intervals most of the time. The unconstrained source model, however, gives a very poor estimate due to its inability to handle gas entering the inversion domain through the input boundary.

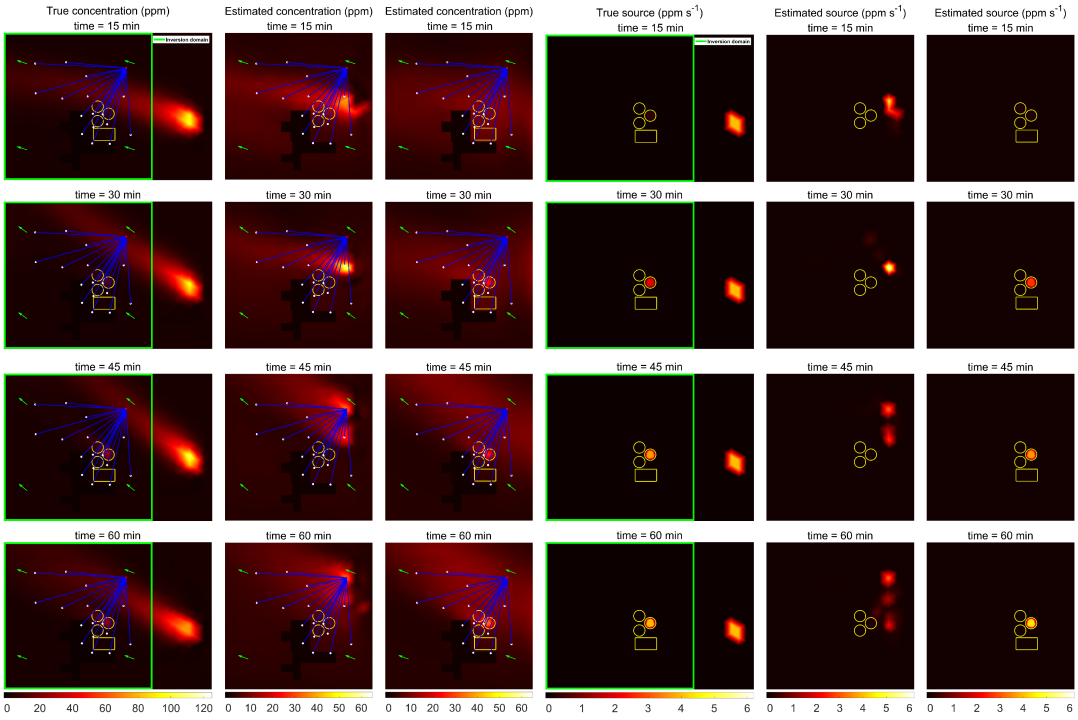

Figure 4. Case 2 - First column) true concentration distribution at different time instants. The green square is the inversion domain. Second column) estimated concentration distribution using the unconstrained model. Third column) estimated concentration distribution using the constrained model. Fourth column) true source distribution. Fifth column) estimated source distribution using the unconstrained model. Sixth column) estimated source distribution using the constrained model.

By comparing the synthetic PAC measurements in Fig. 3 for supplementary case 1 to the PAC measurements in Fig. 5 for supplementary case 2, it can be seen how the external source has contaminated the PAC measurements in case 2. In Fig. 3 for case 1, the peak PAC measurement is $\sim$5 ppm, while the peak PAC measurement for case 3 in Fig. 5 is $\sim$15 ppm. The differences in the PAC measurements are solely due to the external source.

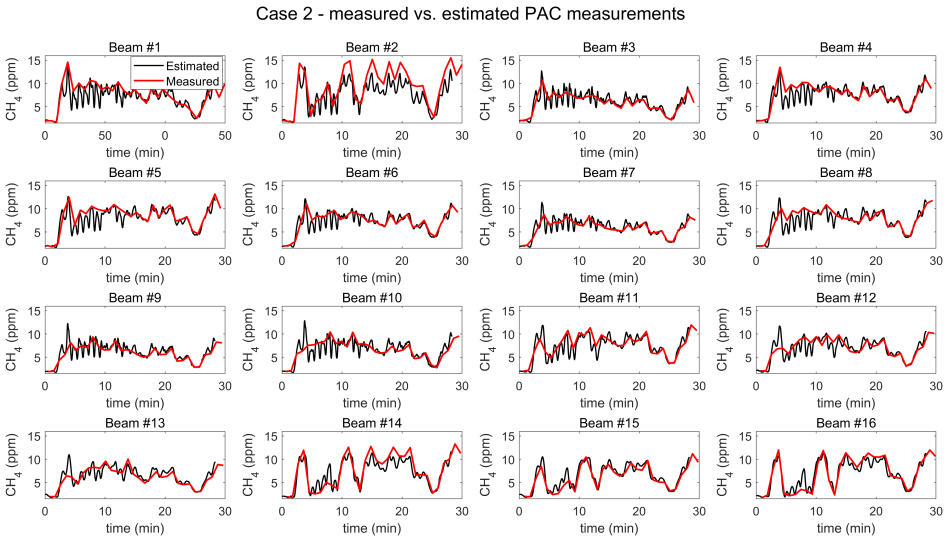

Figure 5. Case 2 - Measured (from forward simulation) and estimated (from inversion) PAC measurements using the constrained model.